Journal of Neurochemistry, 2005, **92**, 1439–1451 doi:10.1111/j.1471-4159.2005.03014.x

Inhibition of microglial inflammation by the MLK inhibitor CEP-1347

Søren Lund,* Peter Porzgen,* Anne Louise Mortensen,* Henrik Hasseldam,* Donna Bozyczko-Coyne,† Siegfried Morath,‡ Thomas Hartung,‡,§ Marina Bianchi,¶ Pietro Ghezzi,¶ Malika Bsibsi,** Sipke Dijkstra** and Marcel Leist*

**H. Lundbeck A/S, Valby, Denmark*

†Cephalon Inc., West Chester, Pennsylvania, USA

‡Biochemical Pharmacology, University of Konstanz, Germany

§ECVAM, Ispra, Italy

¶Mario Negri Institute of Pharmacological Research, Milan, Italy

***TNO Prevention & Health, Leiden, the Netherlands*

Abstract

CEP-1347 is a potent inhibitor of the mixed lineage kinases (MLKs), a distinct family of mitogen-activated protein kinase kinase kinases (MAPKKK). It blocks the activation of the c-Jun/JNK apoptotic pathway in neurons exposed to various stressors and attenuates neurodegeneration in animal models of Parkinson's disease (PD). Microglial activation may involve kinase pathways controlled by MLKs and might contribute to the pathology of neurodegenerative diseases. Therefore, the possibility that CEP-1347 modulates the microglial inflammatory response [tumour necrosis factor-α (TNF-α), interleukin-6 (IL-6), and monocyte chemotactic protein-1 (MCP-1)] was explored. Indeed, the MLK inhibitor CEP-1347 reduced cytokine production in primary cultures of human and murine microglia, and in monocyte/macrophage-derived cell lines, stimulated with various endotoxins or the plaque forming peptide Aβ1–40. Moreover, CEP-1347 inhibited brain TNF production induced by intracerebroventricular injection of lipopolysaccharide in mice. As expected from a MLK inhibitor, CEP-1347 acted upstream of p38 and c-Jun activation in microglia by dampening the activity of both pathways. These data imply MLKs as important, yet unrecognized, modulators of microglial inflammation, and demonstrate a novel anti-inflammatory potential of CEP-1347.

Keywords: Alzheimer's disease, central nervous system, mixed lineage kinase, CEP-1347, inflammation, microglia, TNF-α.

J. Neurochem. (2005) **92,** 1439–1451.

CEP-1347 is a semisynthetic derivative of the indolocarbazole broad kinase inhibitor K-252a (Kaneko *et al*. 1997). It is a potent inhibitor of the mixed lineage kinase (MLK) family and acts biochemically as an ATP site competitor. CEP-1347 potently inhibits all MLKs, for instance with IC_{50} values of 60 nM (MLK1), 80 nM (MLK2) and 40 nM (MLK3) (Maroney *et al*. 2001). The MLKs constitute serine/theonine kinases belonging to the MAPKKK superfamily (Gallo and Johnson 2002). By blocking MLKs, CEP-1347 reduces the activity of the downstream JNK/c-Jun pathway in intact cells with submicromolar potency (Maroney *et al*. 1998; 1999), while it does not block any other member of the MAP kinase family or, for example, protein kinase C (PKC), protein kinase A (PKA) or myosin light chain kinase (Kaneko *et al*. 1997).

Received July 9, 2004; revised manuscript received October 13, 2004; accepted November 10, 2004.

Address correspondence and reprint requests to Søren Lund, Disease Biology, H. Lundbeck A/S, Ottiliavej 9, 2500 Valby, Denmark.
E-mail: sorl@lundbeck.com

Abbreviations used: Aβ, amyloid β; AD, Alzheimer's disease; CNS, central nervous system; COX, cyclo-oxygenase; DMEM, Dulbecco's modified Eagle's medium; FBS, fetal bovine serum; FCS, fetal calf serum; IL-6, interleukin-6; LPS, lipopolysaccharide; LTA, lipoteichoic acid; MAPKKK, mitogen-activated protein kinase kinase kinases; MCP-1, monocyte chemotactic protein-1; MLK, mixed lineage kinase; MTT, 3-(4,5-dimethyl-2-thiazolyl)-2,5-diphenyl-2H-tetrazolium bromide; NF-κB, nuclear factor κB; NO, nitric oxide; PBS, phosphate-buffered saline; PD, Parkinson's disease; PKA, protein kinase A; PKC, protein kinase C; TLRs, toll-like receptors; TNF-α, tumour necrosis factor-α.

© 2005 International Society for Neurochemistry,

Previous experimental work with CEP-1347 has focused on its neuroprotective properties. CEP-1347 has been demonstrated as rescuing dopaminergic neurons in various preclinical models of Parkinson's disease (PD) (Saporito *et al*. 1999; Boll *et al*. 2004), but is also efficacious in rescuing other nerve cell populations such as neurotrophin-deprived sympathetic neurons (Maroney *et al*. 1999; Harris *et al*. 2002). Stressed neurons often undergo apoptosis via activation of the JNK/c-Jun pathway, and the neuroprotective effects of CEP-1347 have been attributed to blockade of this pathway by inhibition of MLKs responsible for the activation of MKK4 and MKK7 (the upstream kinases of JNK) (Xu *et al*. 2001).

Microglial inflammation is a common feature of many neurodegenerative diseases. For instance, autopsies of brains affected by Alzheimer's disease (AD) reveal that activated microglia are consistently found in close proximity with amyloid β (Aβ)-rich plaques, and ample evidence suggests a role of Aβ in microglial activation (Combs *et al*. 2001; Eikelenboom *et al*. 2002; Giovannini *et al*. 2002; McGeer and McGeer 2003). The potential detrimental effect of inappropriately activated microglia in the central nervous system (CNS) is evident from numerous studies where the presence of activated microglia is reported to reduce neuronal viability (Kingham and Pocock 2000, 2001; Gao *et al*. 2002a,b; Munch *et al*. 2003). Also, many compounds that act on microglia, but may also have other actions, have been shown to be beneficial in animal models of neurodegeneration (Kurkowska-Jastrzebska *et al*. 1999; Delgado and Ganea 2003; Yan *et al*. 2003; Hunter *et al*. 2004) and in epidemiological studies (McGeer *et al*. 1990; Chen *et al*. 2003). The causal role of activated microglia in disease enhancement has been extensively reviewed (Gao *et al*. 2003; McGeer and McGeer 2003).

We reasoned that CEP-1347 might act as an alternative, yet unexplored, type of anti-inflammatory agent by virtue of blocking one family of upstream activators of p38 and JNK. Both JNK and p38 have been implicated in macrophage/microglial activation and specific inhibition of either kinase has resulted in anti-inflammatory effects (Nakajima *et al*. 2004; Suzuki *et al*. 2004). JNK and p38 are downstream kinases of several pathways important for cell regulation. Therefore, inhibition of the MLKs would be expected to affect JNK/p38 activation only under certain stressful conditions, but not under all circumstances. In this report the effect of MLK inhibition was tested experimentally by examining different endpoints of microglial inflammation triggered by various inflammatory agents.

Materials and methods

Materials and chemicals

Tissue culture material was obtained from Nunc (Roskilde, Denmark), media, phosphate-buffered saline (PBS), antibiotics, and fetal bovine serum (FBS) were obtained from Gibco (Invitrogen, Taastrup, Denmark). Other reagents were lipopolysaccharide (LPS) (*Salmonella abortus* equi) (BioCloth, Aidenbach, Germany) (*in vitro* use), LPS (*Escherichia coli* 055B:B5) (Sigma, St Louis, MO, USA) (*in vivo* use), amyloid β (Bachem, Bie & Berntsen, Rødover, Denmark), IFN-γ (R & D Systems, Abingdon, UK), and FITC-labelled *E. coli* and lectin from *Bandeiraea simplicifolia* BS-I (Molecular Probes Europe, Leidin, the Netherlands). Aβ1–40 and Aβ40–1 were dissolved in sterile filtered H_20 (4°C) at 1 mM, aliquoted, and stored in sterile Eppendorf tubes at −80°C. Lipoteichoic acid (LTA) from *Staphylococcus aureus* was prepared as earlier described (Morath *et al*. 2001). CEP-1347 was provided by Cephalon Inc. (West Chester, PA, USA). Basic laboratory chemicals were purchased from Sigma unless otherwise stated.

Animals and *in vivo* experimentation

All experimental procedures were carried out in accordance with national (directive of the Danish National Committee on Animal Ethics; Italian D.L. no. 116, G.U., suppl. 40, February 18, 1992) and international laws and policies (EEC Council Directive 86/609, OJ L 358, 1, December 12, 1987; Guide for the Care and Use of Laboratory Animals, US National Research Council, 1996). Pregnant C57bL/6jbom mice were purchased from M & B (Lille Skensved, Denmark). Male, adult CD1 mice were obtained from Charles River, Calco, Como, Italy.

Intracerebroventricular (i.c.v.) injection of LPS

LPS was administered at the dose of 100 ng/mouse, i.c.v., into the lateral ventricle through a 28-gauge needle into ether-anaesthetized mice, as previously described (Lipton *et al*. 1991). Briefly, a 3/8-inch, 28-gauge needle attached to a 0.5-mL allergy syringe was inserted perpendicularly through the skull into the brain. The site of injection was 2 mm from either side of the midline of a line drawn through the anterior base of the ears. All injections were made in 10 μL of sterile, pyrogen-free saline. CEP-1347 was given subcutaneously (s.c.) at a dose of 0.5 or 2.5 mg/kg, 1 h before LPS. Control mice received vehicle alone. Ninety minutes after i.c.v. injections, mice were killed with ether, the brains homogenized in 10 vol. of PBS and the supernatants used for TNF and IL-6 measurements. TNF was measured by the degree of cytotoxicity on L929 cells in the presence of 1 μg/mL of actinomycin D, as previously described (Aggarwal *et al*. 1985), using human recombinant TNF-α as standard; the sensitivity of the assay was 1 U/mL. Serum IL-6 was measured as hybridoma growth factor using 7TD1 cells (a kind gift from Dr van Snick, Brussels) as previously described (Sironi *et al*. 1989). IL-6 activity is expressed as co-stimulatory units/mL using recombinant IL-6 as a standard. The following recombinant cytokines were used to test the specificity of the IL-6 assay, and none was found to have hybridoma growth factor activity on 7TD1 cells: IL-1α and IL-1β; IL-2; IL-3; IL-4; GM-CSF; M-CSF; lymphotoxin, TNF-α and phorbol 12-myristate-13-acetate (PMA). The sensitivity of the assay was 50 U/mL.

Primary human microglia cultures

Microglia were isolated from human white matter samples obtained post-mortem, as previously described (De Groot *et al*. 2000). Briefly, brain tissues dissected from the corpus callosum or subcortical white matter were collected and blood vessels removed. After a 20-min digestion in 0.25% (w/v) trypsine (Sigma) and

0.1 mg/mL Dnase (Boehringer Mannheim, Mannheim, Germany) the cell suspension was gently triturated and washed with Dulbecco's modified Eagle's medium (DMEM)/HAM-F10 medium containing 10% (v/v) fetal calf serum (FCS) and antibiotic supplements. After passage through a 100-μm filter, myelin was removed by Percoll gradient centrifugation. Erythrocytes were lysed by a 15-min incubation on ice with 155 mM NH_4Cl, 1 mM $KHCO_3$, 0.2% (w/v) bovine serum albumin (BSA). The remaining cell suspension was collected by centrifugation and resuspended in culture medium (DMEM/HAMF10 medium containing 10% (v/v) FCS and antibiotic supplements). For this study, cells were seeded in 12-well plates. After 3–5 days, the medium was changed and recombinant human granulocyte-macrofage colony stimulating factor (rhGM-CSF, PeproTech Inc, Rocky Hill, NJ, USA) was added to the microglial cultures at a final concentration of 10 ng/mL. This was repeated twice a week until cultures were ready for stimulation.

Primary murine microglia culture

Pregnant C57bL/6jbom mice were purchased from M & B (Lille Skensved, Denmark). Microglia cultures were prepared as initially described by Giulian and Baker (1986) using the following adaptations: pups (1–3 days post-partum) were decapitated and the cerebra were transferred to DMEM with 20% heat inactivated FBS, supplemented with antibiotics (penicillin 100 U/mL, streptomycin 100 μg/mL). This medium was used for all work related to primary microglia; only the FBS concentration was varied. Following removal of meninges, brains were triturated with a 10-mL pipette to obtain a homogeneous cell suspension that was subsequently passed though a 70-μm cell strainer (sieve) into 50-mL test tubes. The cell suspension was plated at a density of three brains/185-cm^2 flask and cultured undisturbed for 7 days. Then, new medium with reduced serum concentration (10% FBS) was added. After seven additional days of culturing, microglial cells were selectively detached by shaking (300 r.p.m., 1 h). Suspended microglia were pelleted at 180 *g*, before being seeded. Purity was always > 90% as determined by routine staining with FITC-labelled lectin from *Bandeiraea simplicifolia* BS-I.

Standard cell incubation scheme

All incubation was performed at 37°C, 5% CO_2, 95% relative humidity. Suspended primary microglia (see above) were seeded at 20 000 cells/well (100 μL media) in 96-well plates. After 25 min of incubation, loosely adherent cells were removed by tapping the sides of the plate, followed by two washes. After overnight incubation, cells were washed once in PBS followed by addition of 100 μL medium (1% FBS). CEP-1347 was added 45 min before LPS stimulation, and kept in aliquots [−20°C, 10 mM, dimethylsulfoxide (DMSO)] that were maximally thawed twice. Compounds were added in volumes of 10% of the total well volume. The final DMSO concentration was 0.005% and did not affect the endpoints measured. Following LPS (100 ng/mL) stimulation for 8, 12 or 24 h, 50 μL of the supernatant was sampled for cytokine analysis. After 24 h total incubation, viability was measured with the 3-(4,5-dimethyl-2-thiazolyl)-2,5-diphenyl-2H-tetrazolium bromide (MTT) reduction assay. A similar set-up was used for measurement of nitrite, except that IFN-γ (10 U/mL) was included as a co-stimulus, and the stimulation period was extended to 24 h.

MTT reduction assay (cell viability measure)

Medium was aspirated and replaced with new medium containing 0.5 mg/mL MTT. After 2 h of incubation, medium was aspirated, and the precipitated formazan was dissolved in 100 μL formic acid (5%)/isopropanol (95%). Absorbance was read at (550–690 nm).

Cell line maintenance

BV-2 cells [murine microglia, kindly provided by E. Blasi, Perugia (Blasi *et al.* 1990)] were maintained in RPMI supplemented with 10% FBS and antibiotics (penicillin 100 U/mL, streptomycin 100 μg/mL). The cell lines RAW264.7 (origin, murine macrophage) and THP-1 (origin, human monocyte) were both obtained from American Type Culture Collection (Rockville, MD, USA) (TIB-71 and TIB-2002, respectively). Both cell lines were maintained in DMEM supplemented with 10% FBS, and antibiotics (penicillin 100 U/mL, streptomycin 100 μg/mL). The THP-1 medium was further supplemented with 0.05 mM 2-mercaptoethanol.

During experiments the cell lines were incubated with their respective media containing only 1% FBS. Cells were plated in Petri dishes (for western blot and gene array analysis at 25% confluency) or 96-well plates (15 000 cells/well) 1 day in advance of an experiment. The following day, the cells were washed once in PBS, the medium was replaced (1% FBS), and the cells were stimulated.

Nitrite/cytokine measurements

Nitrite [surrogate marker for nitric oxide (NO)] was measured by use of the Griess reagent. In brief, 100 μL supernatant or $NaNO_2$ standards were mixed with 10 μL *N*-(1-naphtyl) ethylendamine (0.1% in H_2O) and 10 μL sulfanilamide (1% in 1.2 N HCl) in a 96-well plate. After 3 min, samples were read at (570–690 nm) in a spectrophotometer.

The murine cytokines interleukin 6 (IL-6), monocyte chemotactic protein 1 (MCP-1) and tumour necrosis factor-α (TNF-α) were measured using murine specific OptEIA™ ELISA kits from Pharmingen (Brøndby, Denmark) in MaxiSorp plates from Nunc. TNF-α from human cultures was measured using PeliKine Compact Human TNF-α ELISA kit obtained from Sanquin (Amsterdam, the Netherlands).

Western blot analysis

BV-2 cells were washed once in PBS before lysis in ice-cold buffer containing 1% NP-40, 20 mM Tris-HCl pH 8.0, 137 mM NaCl, 10% glycerol, 4 mM iodo acetamide, 10 mM NaF, 1 mM AEBSF, 1 mM Na_3VO_4 and 'Complete mini' protease-inhibitor mix from Roche (1 pill/10 mL buffer). The lysate was transferred to a microfuge tube and incubated for 15 min on ice before cellular debris was spun down for 10 min at 18 000 *g* at 4°C. The supernatants were transferred to a fresh tube and stored at −80°C. The protein concentration was determined by the bicinchoinic acid (BCA) method using a commercial kit from Pierce (Rockford, IL, USA). The NuPAGE-kit (4–12% Bis-Tris gel run with MOPS buffer under reducing conditions) from Invitrogen was used for electrophoresis (20 μg protein per lane) according to the manufacturer's instruction. Gels were run for approximately 1 h at 200 V before proteins were blotted onto an activated polyvinylidene difluoride (PVDF) membrane (Immobilon P, Millipore, Glostrup, Denmark) using wet-transfer blot module XCell2 from Invitrogen. Membranes were blocked with 5% milk powder in TBS/T (2.42 g/L Tris base,

8 g/L NaCl, and 1% Tween-20 pH 7.6) and incubated with primary antibody dissolved in either 5% milk powder or 4% bovine serum albumin in TBS/T overnight at 4°C. Blots were washed and incubated with appropriate horseradish peroxidase-conjugated secondary antibodies [rabbit anti-mouse and goat anti-rabbit, both diluted 1 : 1,000 and both from Dako (Glostrup, Denmark)] for 2 h at room temperature (21°C), and developed using ECL or ECL+ (Amersham Pharmacia Biotech, Piscataway, NJ, USA). Primary antibodies (IgG) against phosphorylated-c-Jun (P-c-Jun) and phosphorylated-JNK (P-JNK) were from Santa Cruz Biotechnology, (Santa Cruz, CA, USA). Primary antibodies against P-p38, and IκBα were from Cell Signaling Technology (Beverly, MA. USA) but purchased though Medinova Scientific A/S (Hellerup, Denmark). Primary antibody against p-MLK3 was from Biosource, purchased through AH Diagnostic (Aarhus, Denmark). All primary antibodies were used in a dilution of 1 : 1000. To verify equal amounts of protein loading, the membranes were stripped and reprobed with an antibody for β-actin (Chemicon, AH Diagnostic AS, Aarhus, Denmark). For stripping, the membranes were sealed in a plastic bag with 15 mL of a stripping buffer [2% sodium dodecyl sulfate (SDS), 50 mM Tris-HCL and 100 mM 2-mercaptoethanol] and incubated for 25 min at 55°C in a water bath.

Nuclear translocation/intensity of NF-κB and c-Jun

For quantification of nuclear factor κB (NF-κB) translocation and c-Jun nuclear intensity, cells were plated at 20 000 cells/well in DMEM with 1% FBS. After overnight incubation, the cells were stimulated with 100 ng/mL of LPS (*S. abortus*) and then fixed with 10% paraformaldehyde for 10 min. The cells were stained according to the manufacturer's instruction. Antibody kits were purchased from Cellomics™ though Ramcon (Birkerød, Denmark). The primary antibody recognized, respectively, NF-κB (p65) or P-c-Jun, and the binding was visualized with an FITC-labelled secondary antibody. Cells were counterstained with H-33342 and the nuclear translocation/intensity of NF-κB and c-Jun was quantified with a Cellomics ArrayScan™, using the pre-defined algorithm 'cytoplasm to nucleus translocation'. The principle is based on cell image acquisition with a high-resolution CCD camera, followed by automatic identification of cells (based on nuclear staining with H-33342). The nuclear-cytoplasmic difference in antigen-signal intensity was quantified by subtracting the antigen-intensity of the area between the nucleus and a circle created two pixels towards the plasma membrane (measured from the nuclear perimeter) from the antigen-intensity in the nucleus (defined as antigen pixels overlapping H33342 positive pixels).

Real-time PCR

Cells stimulated in 10-cm dishes were washed once with PBS and total RNA was extracted using TRIzol reagent (Invitrogen) according to the manufacturer's protocol. DNA-free™, Dnase-1 kit was purchased through (Ambion, Huntingdon, UK) and the purified RNA was treated according to the manufacturer's protocol. Total RNA (1 μg) was reverse transcribed with TaqMan RT-Reagent (Applied Biosystems, Nærum, Denmark), using random hexamers in a 100-μL reaction on a PTC-200 DNA Engine Thermal Cycler (VWR international, Albertslund, Denmark), using a programme of 10 min annealing at 25°C, 30 min reverse transcription at 48°C, 5 min inactivation at 95°. The cDNA was quantified using the SYBR GREEN® PCR Master Mix kit (Applied Biosystems, Nærum, Denmark). Each reaction contained 2.5 μL cDNA of the 100 μL RT-product, 300 nM forward and reverse primers, 12.5 μL master mix and 7 μL water in a total volume of 25 μL. PCR amplification was run in a 96-well experimental plate format on an iCycler Thermal Cycler equipped with iCycler Optical System (Bio-Rad, Hercules, CA, USA). The programme set-up was 10 min at 95°C, 40 cycles of 15 s at 95°C/1 min at 60°C. A melting curve was obtained to verify the measured signal and the product was run on a 4% agarose gel to verify the presence of only one amplified band. Quantification was performed as follows: using the iCycler data analysis software (Bio-Rad), the threshold cycle (C_T) was determined for each sample. C_T was defined as the cycle at which the level of fluorescence increased linearly. Each sample was run in two reactions, one with the primer set of interest and one with a GAPDH primer set. The mRNA levels were compared among groups using the delta-delta method as described by Dr Margaret Hunt (http://www.med.sc.edu:85/pcr/realtime-home.htm). All primers, except the housekeeping gene GAPDH, were intron-spanning in order to distinguish cDNA from genomic DNA. Primers were designed using DNA-star software package (DNASTAR Inc, Madison, WI, USA) and scrutinized to minimize secondary structures, self-complementarity, optimal melting temperature, etc. All primers were blasted using BLASTn to ensure primer specificity for the gene of interest (http://www.ncbi.nlm.nih.gov/BLAST/). Primers used were GAPDH sense (NM_008084): 5′-TGCACCACCAACTGCTTAG-3′, antisense: 5′-GGATGCAGGGATGATGTTC-3′; tnf sense (NM_013693): 5′-CTATGGCCCAGACCCTCACACTCA-3′, antisense: 5′-CACTCCAGCTGCTCCTCCACTTG-3′; upa sense (NM_008873): 5′-AGGTTTACTGATGCTCCGTTTGGTTC-3′, antisense 5′-TTTACGACGGACATTTTCAGGTTCTTT-3′; mcp-1 sense (NM_011333): 5′-CATGCTTCTGGGCCTGCTGTTC-3′, antisense 5′-CCTGCTGCTGGTGATCCTCTTGTAG-3′; mip-1α sense (NM_002983): 5′-CCCGACTGCCTGCTGCTTCTC-3′, anti sense: 5′-GATCTGCCGGTTTCTCTTAGTCA-3′; socs3 sense (NM_003955): 5′-ACTTGTTTGCGCTTTGATTTGGTTT-3′, antisense: 5′-GTTGGGCAGTGGGAGTGGTTATTT-3′; IL-6 sense (NM_000600.1): 5′-GGAGCCCACCAAGAACGATAGTCA-3′, antisense: 5′-GAAGTAGGGAAGGCCGTGGTTGTC-3′.

Transcript analysis by oligonucleotide hybridization analysis

A shortlist of mouse cytokines and inflammatory factors was compiled. For each of these genes, one oligonucleotide (40–50 mer) was designed by MWG (MWG, Ebersberg, Germany) using their proprietary Oligo4array software and CodeSeq database, which selects the oligos preferentially from the 3′-region of each coding sequence. Furthermore, each oligomer was scrutinized to meet physicochemical parameters (like melting temperature, self-complementarity, secondary structure, etc.) and extensively tested to minimize cross-hybridization to other sequences of the mouse genome in silico. All oligos were synthesized using MWG's HPSF technology followed by MALDI-TOF quality control.

The oligomeres were spotted onto activated glass slides (Pan Epoxy, MWG or CodeLink, Amersham) using a 417 Affymetrix (ring and pin) spotter. Sample preparation and labelling was carried out as described by Joseph DeRisi (http://www.microarrays.org/protocols.html), a protocol, derived from Hughes *et al*. (2001). In brief: 12–15 μg of total RNA were reverse transcribed using random

hexamere and dT16 primers and Superscript II reverse transcriptase (Invitrogen), incorporating amino-allyl dUTP into the 1st-strand cDNA. After the cDNA synthesis, the remaining RNA was hydrolyzed and after a clean-up step (Microcon-30 spin filters, Millipore), Cy-3 or Cy-5 dye esters, respectively, were coupled to the cDNA samples. Excessive dye and buffer were removed with QiaQuick PCR purification columns (Qiagen, Valencia, CA, USA) and the eluates were concentrated with Microcon-30 spin filters. The hybridization mixture contained the Cy-labelled cDNAs in hybridization buffer [50% formamide, 6 × saline sodium citrate buffer (SSC), 5 × Denhardts, 0.5% SDS and 50 mM sodium phosphate, pH = 8] and was denatured for 5 min before incubation on the slides for 16 h at 42°C. Washing was carried out in three steps of increasing stringency: 2 × SSC, 0.1% SDS followed by 1 × SSC, 0.01% SDS and 0.5 × SSC (all solutions were pre-heated to 30°C). Finally, each slide was spun dry and scanned in a 428 Affymetrix confocal laser scanner at three different intensities (photo multiplier gains).

The microarrays were analyzed using ImaGene 4.2 (BioDiscovery) for spot location, array alignment and background subtraction. Signal intensities for individual spots were adjusted for local background. Microsoft Excel was used for further statistical analysis of the ImaGene output files. For example, Cy3/Cy5 ratio normalization was carried out by multiplying each ratio value with a scaling factor, which was defined as the ratio of the overall signal intensity of the Cy5 versus Cy3 channel (Knudsen 2002). Each microarray experiment was performed at least twice independently. To further account for bias introduced by dye bleaching or labelling, each experiment was carried out as dye-swap experiment with the resulting ratio value being the arithmetical mean from two slides of opposite labelled sample pairs. Genes with very low signal intensities (less than eightfold of the background) were excluded from the analysis. Data were deposited at the MIAME website and are also freely accessible at http://www.public-results.com.

Phagocytosis assay

Determination of microglia phagocytosis was performed as described previously (Lehner *et al*. 2002). Briefly, 20 000 primary microglia/well (100 μL/well, 10% FBS) were plated in a 96-well microtitre plate. The following day, cells were washed once in PBS, and then incubated in medium (1% FBS) with increasing concentrations of CEP-1347. After 45 min, sonicated tetramethylrhodamine-conjugated fluorescent *E. coli* particles were added to a final concentration of 50 μg/mL. After 4 h of stimulation, supernatants were sampled for cytokine analysis, and phagocytosis was stopped by washing the cells twice with PBS to remove non-phagocytosed bacteria. Cells were then lysed by addition of 100 μL/well of PBS with 20 mM HEPES + 0.2% Triton X-100. Fluorescence was determined at 530 nm excitation and 590 nm emission wavelengths using a fluorescence microplate reader (Labsystem, Finland). Cells without bacteria were used to determine the background fluorescence.

Results

Modulation of LTA- and LPS-induced microglial inflammatory responses by CEP-1347

In neurodegenerative diseases, microglia are transformed from a resting to an activated state by poorly characterized stimuli. A small battery of standard inflammatory stimuli (Aβ1–40, bacteria, LPS and LTA) was therefore included to examine the potential effect of the MLK inhibitor CEP-1347 on inflammatory activation. As representative endpoints for inflammation, the release of TNF-α, IL-6 and MCP-1 was measured. First, it was investigated whether primary microglia activated via the toll-like receptors (TLRs) were susceptible for modulation by CEP-1347. Therefore, cells were stimulated with the TLR-4 agonist LPS, or the TLR-2 agonist LTA, to trigger cytokine production. Pre-incubation with CEP-1347 (0–500 nM) resulted in a significant inhibition of cytokine and chemokine production (TNF-α, IL-6, MCP-1) at drug concentrations ≥250 nM (Figs 1a–c). Inhibition of cytokine release in LPS-stimulated BV-2 cells followed a similar concentration-dependent relationship, but with more potent inhibition by CEP-1347 (Fig. 1d). BV-2 cells were also found to respond to LTA with cytokine production that paralleled primary microglia, and the cytokine response was dose-dependently inhibited by CEP-1347 (data not shown). The cellular viability was carefully monitored to ensure that the modulation was unrelated to toxicity. Cells tolerated CEP-1347 well over a 24-h period. The data demonstrate that MLK inhibition by CEP-1347 results in inhibition of cytokine production induced by activation of receptors belonging to the toll-like receptor family.

General anti-inflammatory effects of CEP-1347

Next, it was investigated whether CEP-1347 had an anti-inflammatory effect when cells were stimulated with a TLR-2/4 independent stimulus. For this purpose, the Aβ peptide

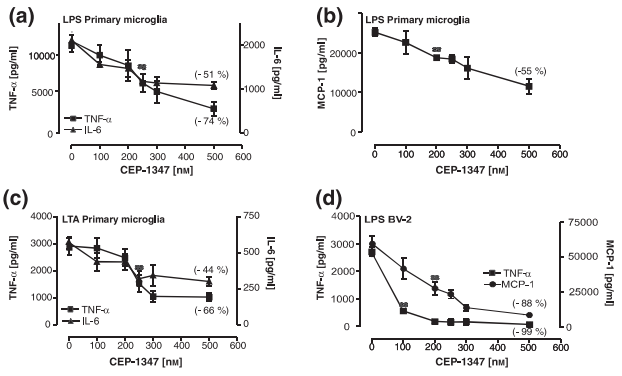

Fig. 1 Modulation of endotoxin-induced expression of inflammatory mediators by CEP-1347. Primary microglia (a, b, c) or BV-2 cells (d) were pre-treated for 45 min with CEP-1347 and then stimulated with LPS (100 ng/mL) (a, b, d) or LTA (3 μg/mL) (c). After 8 h (TNF-α, IL-6) or 12 h (MCP-1) an aliquot of the supernatant was sampled for cytokine analysis. Viability was measured 24 h after stimulation (MTT reduction assay) and was not affected. Data are displayed as means ± SD of triplicates. Experiments were performed three times, and one representative data set is shown. **First significant datapoint with $p < 0.01$.

was chosen because of its potential activation of microglia in AD. Stimulation of RAW264.7 cells for 16 h with the Aβ1–40 peptide induced release of TNF-α and the effect was enhanced with IFN-γ as a co-stimulus. Stimulation with IFN-γ or the reverse sequence of Aβ (Aβ40–1) did not result in any TNF-α production above background. A similar response to Aβ was established for BV-2, and primary microglia cells, although the maximally induced production of TNF-α was modest (~100 pg/mL) compared with the RAW cells (~2000 pg/mL). Also in this experimental set-up, pre-incubation with CEP-1347 concentration dependently reduced TNF-α production (Fig. 2a). Exposure to Aβ1–40 itself resulted in reduced viability values, but the toxicity was strictly Aβ-dependent as cells treated with Aβ together displayed the highest concentration of CEP-1347 equivalent viability values to cells treated with Aβ alone (data not shown). To investigate if the effect of CEP-1347 could also be observed in human cells, first the monocytic cell line THP-1 was stimulated with LPS to induce TNF-α production. CEP-1347 was found to inhibit TNF-α production with an IC_{50} value of approximately 100 nM (Fig. 2b). Then, the effect of CEP-1347 was validated in human primary microglia from two different donors. CEP-1347 reduced LPS induced TNF-α production at concentrations as low as 100 nM in both donors (Fig. 2c). The results indicate that members of the MLK family, across species, are involved in the transmission of inflammatory signals.

Reduction of TNF-α release by CEP-1347 without suppression of phagocytosis capacity or prevention of iNOS induction

We examined whether CEP-1347 would inhibit other features characteristic of activated microglia. A typical, alternative readout is the production of NO. When primary microglia were stimulated with either LPS or LTA + IFN-γ, pre-incubation with a high concentration (500 nM) of CEP-1347 inhibited NO production only marginally by a maximum of 15–25% (Fig. 3a). The NO release data were further supported by the observation that the induction of inducible nitric oxide synthetase (iNOS) by LPS or LTA was unaffected by CEP-1347 (Fig. 3b). Similar findings were made for BV-2 cells, where pre-incubation with 500 nM of CEP-1347 reduced NO production by ~15% when the cells were exposed to the stimuli described above. It therefore appears that CEP-1347 selectively inhibits the release of some cytokines, but does not generally blunt the response of microglia to pathogens. To exploit this further, fluorescently labelled *E. coli* were added to primary cultures of microglia or BV-2 cells to correlate MLK inhibition with both TNF-α production and the phagocytic capability. Pre-incubation with CEP-1347 (0–500 nM) did not affect phagocytosis, but concentration dependently reduced TNF-α production (Fig. 3c) (data for BV-2 cells not shown). Cytochalasin B (10 μM), which is an inhibitor of phagocytosis (inhibits actin

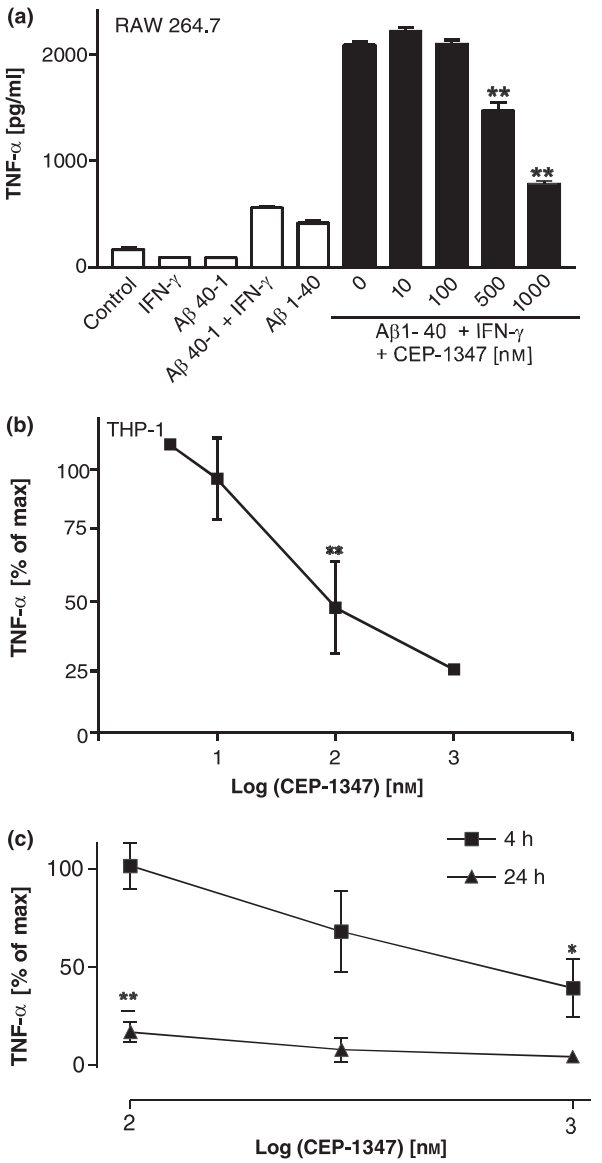

Fig. 2 General anti-inflammatory effect of CEP-1347. RAW264.7 cells (a), THP-1 cells (b) or human microglia (c) were pre-incubated with increasing concentrations of CEP-1347 for 45 min. Then, the RAW264.7 cells were stimulated with Aβ1–40 (20 μM) + IFN-γ (10 U/mL) for 16 h. The reverse sequence, Aβ40–1 (20 μM) + IFN-γ (10 U/mL), was included as negative control to the correct Aβ sequence. THP-1 cells were stimulated with LPS (1 μg/mL) for 4 h, and the human microglia were stimulated with LPS (200 ng/mL) for both 4 and 16 h. Following stimulation, supernatant was sampled for cytokine measurement and viability was regularly controlled by the MTT reduction assay. Statistics were performed by comparing stimulated cells to cells receiving both the stimulus and CEP-1347 treatment (one-way ANOVA test). Data for RAW 264.7 and THP-1 cells are displayed as means ± SD of triplicate determinations. The experiments were performed three times, and one representative data set is shown. For data related to human microglia, each data point represents the average of four measurements obtained from two donors ± SEM. First significant data point with $p < 0.01$ (*) and $p < 0.05$ (**).

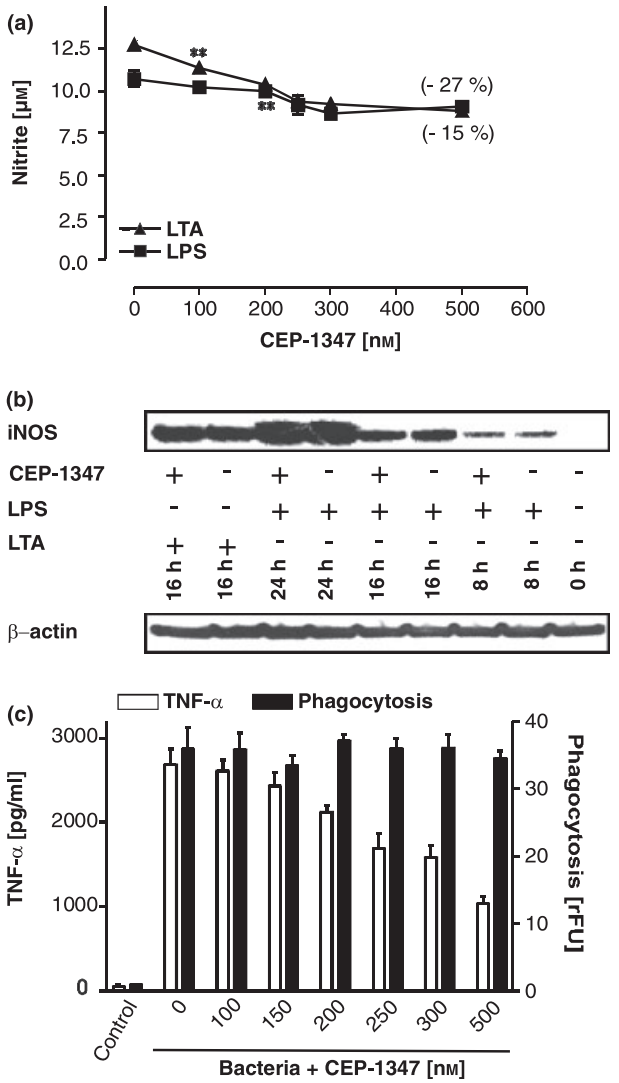

Fig. 3 Differential modulation of microglia activation by CEP-1347. (a) Primary microglia were pre-incubated with increasing concentrations of CEP-1347 for 45 min, followed by stimulation with either LPS (100 ng/mL) + IFN-γ (10 U/mL) or LTA (3 μg/mL) + IFN-γ (10 U/mL) for 24 h. Viability was measured 24 h after stimulation (MTT reduction assay) and was not affected. (b) Primary microglia were pre-incubated ± CEP-1347 (500 nM) for 45 min, followed by stimulation with LPS (100 ng/mL) + IFN-γ (10 U/mL) and LTA (3 μg/mL) + IFN-γ (10 U/mL) for various time points before cell lysis. The intracellular expression level of iNOS was evaluated by western blot analysis. To ensure equal protein loading, the membranes were stripped and re-probed with a β-actin specific antibody. (c) Primary microglia were pre-treated with increasing concentrations of CEP-1347 for 45 min and then fluorescent *E. coli* (50 μg/mL) were added. After 4 h of incubation, TNF-α released to the supernatant was measured and the phagocytosis index was determined. Experiments for phagocytosis and nitrite production were performed six times, and one representative data set is shown. Induction of iNOS was analyzed once. Data are displayed as means ± SD of triplicate determinations.

polymerization) was included in the experiments, and reduced the intake of bacteria by 50% (data not shown). The results demonstrate that, within the same experimental set-up, CEP-1347 spares the machinery for phagocytosis while it inhibits TNF-α production induced by *E. coli*.

Effects of CEP-1347 on MAPK signalling in microglia

Microglial activation is described in the literature as involving phosphorylation of JNK/c-Jun and p38 (Kim *et al.* 2004) and, to investigate if our experimental system gave similar results, BV-2 cells were stimulated with LPS. As expected, the phosphorylation of p38 and JNK was strongly increased upon activation of microglia cells. Whereas the activation of JNK and p38 appeared as a brief pulse (30–120 min) after LPS stimulation, the phosphorylation of the transcription factor c-Jun was more prolonged (30–360 min). Pre-incubation with CEP-1347 reduced phosphorylation of all three proteins at all time points (Fig. 4). The results strongly suggest that LPS-mediated microglial activation involves MLK activity and corroborates the notion that MLKs act upstream of both the JNK and p38 pathway in activated microglia.

Effect of CEP-1347 on nuclear translocation of NF-κB and on nuclear P-c-Jun

Stimulation of microglia results in the activation of the transcription factors NF-κB and c-Jun which control the expression of mRNA for inflammatory mediators (Dukic-Stefanovic *et al.* 2003). To investigate if the anti-inflammatory mechanism of CEP-1347 was associated with either of the above processes, the nuclear translocation of NF-κB and the amount of nuclear P-c-Jun were investigated for primary microglia stimulated with LPS. Cells were stained for the respective antigen, digitally imaged and analyzed with an algorithm to quantify cytosolic and nuclear staining intensity.

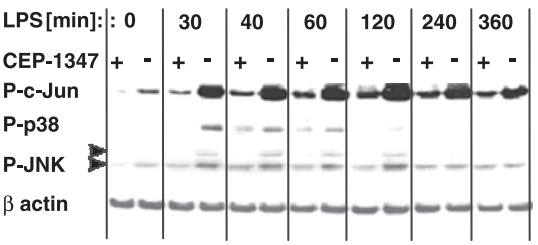

Fig. 4 Activation of MAPK in microglial cells by LPS and inhibition of activation by CEP-1347. BV-2 cells were pre-incubated with CEP-1347 (0 or 500 nM) and stimulated with LPS (100 ng/mL). At the indicated times, the phosphorylation state of JNK, p38, and c-Jun was determined by western blot with phospho-specific antibodies. Arrows indicate JNK bands at 46 and 55 kDa. To control for protein loading, the membranes were stripped and re-probed with a β-actin specific antibody (one representative loading control is shown). One representative blot of two is shown.

The LPS induced increase in phosphorylation of c-Jun was manifested as a rapid (30–60 min) increase of the nuclear staining intensity, and was significantly reduced by pre-treatment with CEP-1347 at all time points (Fig. 5a). This observation from primary microglia fully corroborates the findings with CEP-1347 regarding c-Jun phosphorylation in LPS-stimulated BV-2 cells (Fig. 4).

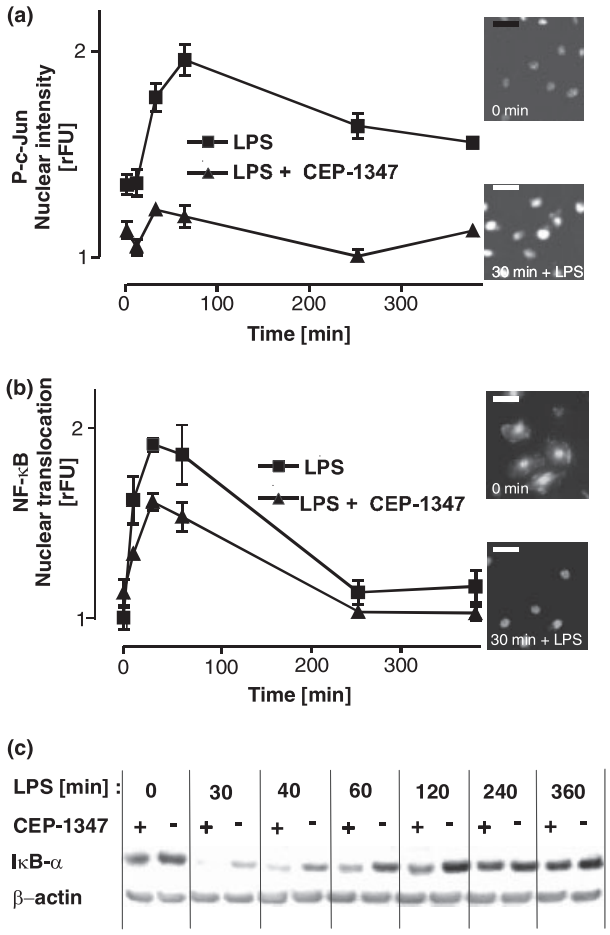

Fig. 5 Differential effects of CEP-1347 on the LPS-induced activation of NF-κB and P-c-Jun by CEP-1347. Primary microglia were stimulated with LPS (100 ng/mL) for the indicated times [± pre-incubation with CEP-1347 (500 nM) for 45 min]. The effect of the MLK inhibitor on (a) nuclear intensity of P-c-Jun and (b) NF-κB translocation was assessed by immunocytochemistry using image software capable of quantifying the fluorescent intensity in the nucleus and the cytosol, respectively. At least 50 fields were imaged per data point and data are displayed as means ± SD of triplicates. Inserts show typical immunocytochemical stains used for the automatic quantification of P-c-Jun and NF-κB. Scale bar = 20 μm. (c) The degradation of NF-κB inhibitor protein α (IκB-α) was monitored in BV-2 cells by western blot analysis, and equal protein loading was verified with a β-actin-specific antibody. Experiments for NF-κB and c-Jun activation were performed three times, and one representative data set is shown. Degradation of IκB-α was examined twice, and one representative blot is shown.

The nuclear translocation of NF-κB, as measured by immunocytochemistry, was maximal at 30 min, and then declined slowly over 4 h upon LPS stimulation (Fig. 5b). Pre-treatment with a high concentration of CEP-1347 (500 nM) hardly reduced the nuclear translocation of NF-κB, and the lack of effect on NF-κB was reflected in largely unchanged regulation of IκB-α at the protein level (Fig. 5c). LPS was also found to induce phosphorylation of MLK3 which, as expected, was unaffected by CEP-1347 pre-treatment (data not shown). Overall, it appears that CEP-1347 targets mainly the P-c-Jun pathway and spares the NF-κB system.

Transcriptional regulation of inflammatory mediators by CEP-1347

In order to gain further insight into the differential regulation of the inflammatory response by CEP-1347, we took advantage of a small custom-spotted oligonucleotide array containing probes relevant to inflammation. RNA was purified from LPS stimulated BV-2 cells after 4 h (± CEP-1347 pre-treatment) and expression levels of mRNA were compared by competitive hybridization. The early time point was chosen to ensure that mainly direct regulations, and not secondary effects, were detected. Regulations were considered significant when the regulation was ≥ 1.7-fold in at least five out of six hybridization experiments performed. Because of these stringent conditions, LPS was found to robustly up-regulate only the following genes corresponding to: (i) secreted factors (serum amyloid a2, mip-1β, mip-1α, serum amyloid a3, plasminogen activator inhibitor, bdnf, mcp-1), (ii) inflammatory surface markers (toll-like receptor 2, intercellular-adhesion molecule-1 (icam1), glycoprotein 49a, tnfrsf5), (iii) a kinase (cyclin-dependent kinase 7), (iv) transcription factors and their regulators (ccaat/enhancer binding protein, i(κ)b(α), p50/p105, p49/p100, pu.1), (v) intracellular modulators of inflammation (socs3, lipocalin 2), and (vi) apoptosis-related genes (caspase 9, caspase 4/11). Not up-regulated at this time point were, for example, inos, and matrix-metalloproteinase 9. To examine the regulation by CEP-1347, RNA from cells stimulated with LPS was competitively hybridized against RNA from cells stimulated with LPS + CEP-1347. Of genes belonging to the class of secreted factors that were up-regulated by LPS, CEP-1347 was found to counter-regulate most of the cytokine genes. The expression of the anti-inflammatory plasminogen activator inhibitor gene was not down-regulated and the expression of serum amyloid a2, and serum amyloid a3, was even enhanced. Of other genes up-regulated by LPS, CEP-1347 counter-regulated glycoprotein 49a, and caspase 9, while it enhanced the transcription level of ccaat/enhancer binding protein and lipocalin 2. Finally, CEP-1347 down-regulated three genes not regulated by LPS (atf3, c-jun, u-pa) while it enhanced the LPS-induced down-regulation of regulator of G-protein signalling 2 (rgs2).

In order to confirm the differential hybridization data, real-time PCR was performed for four selected genes. The expression level of socs3 was confirmed as not being down-regulated by CEP-1347 in LPS-stimulated cells, whereas the mip-1α, u-pa and mcp-1 levels were confirmed as being significantly reduced (Figs 6b–e). A functional oligo for tnf-α was not on the array, but real-time PCR showed both significant up-regulation by LPS and down-regulation by CEP-1347 pre-treatment (Fig. 6f). The hybridization signal (detection factor) for Il-6 did not exceed the selected intensity threshold, but Il-6 transcription was confirmed by real-time PCR as being up-regulated by LPS and counter-regulated by CEP-1347 (Fig. 6g).

Anti-inflammatory effects of CEP-1347 in a mouse model for cerebral inflammation

After having established anti-inflammatory effects of CEP-1347 *in vitro*, the compound was examined *in vivo* in a model for cerebral inflammation. Pre-treatment of CD1 mice for 1 h with CEP-1347 (0.5 and 2.5 mg/kg) significantly reduced the production of TNF after i.c.v. injection of LPS, and showed a tendency towards inhibition of IL-6 production (Fig. 7). The results for *in vivo* inhibition of TNF production indicate that the anti-inflammatory action described for CEP-1347 *in vitro* can be directly transferred to the more complex CNS environment where microglia interact with multiple other cell types.

Discussion

Previous experimental work with CEP-1347 has focused on its direct neuroprotective effects in various preclinical models but has not addressed microglial inflammation. The present work emphasizes CEP-1347 as a modulator of cytokine production in activated microglia.

(a)

	Average ratio LPS vs control	Average ratio LPS vs LPS/CEP-1347	Gene Bank number
Secreted factors			
serum amyloid a 2	13.9	0.5	NM_011314
mip-1 beta	7.0	9.4	NM_013652
mip-1alpha	6.1	3.6	NM_011337
serum amyloid a 3	5.4	0.5	NM_011315
pai-1, plasminogen activator inhibitor	3.0	1.1	NM_008871
bdnf	1.7	1.8	NM_007540
mcp-1	1.7	1.9	NM_011333
u-pa, plasminogen activator, urokinase	0.9	3.2	NM_008873
Inflammatory plasma membrane markers			
toll-like receptor 2	6.7	0.8	BC014693
icam1	3.4	0.8	NM_010493
glycoprotein 49a	2.8	2.2	NM_008147
tnfrsf5	2.4	1.1	NM_011611
Kinases			
cyclin-dependent kinase 7	4.1	1.2	XM_127539
Transcription factors or and their regulators			
ccaat/enhancer binding protein	5.3	0.5	NM_009883
i(kappa)b(alpha)	5.2	1.0	NM_010907
p50/p105, nfkb1	2.3	1.0	NM_008689
p49/p100, nfkb2	2.2	0.9	NM_019408
pu.1	2.0	1.1	NM_011355
atf3, activating transcription factor 3	1.4	2.6	NM_007498
ap-1, c-jun	0.9	1.8	BC032086
Intracellular modulators of inflammation			
socs3	3.1	0.9	BC052031
lipocalin 2	2.1	0.4	XM_130171
rgs2, regulator of g-protein signaling 2	0.3	4.8	NM_009061
Apoptosis related genes			
caspase 9	4.8	3.1	NM_015733
caspase 4/ caspase 11	3.4	0.8	NM_007609

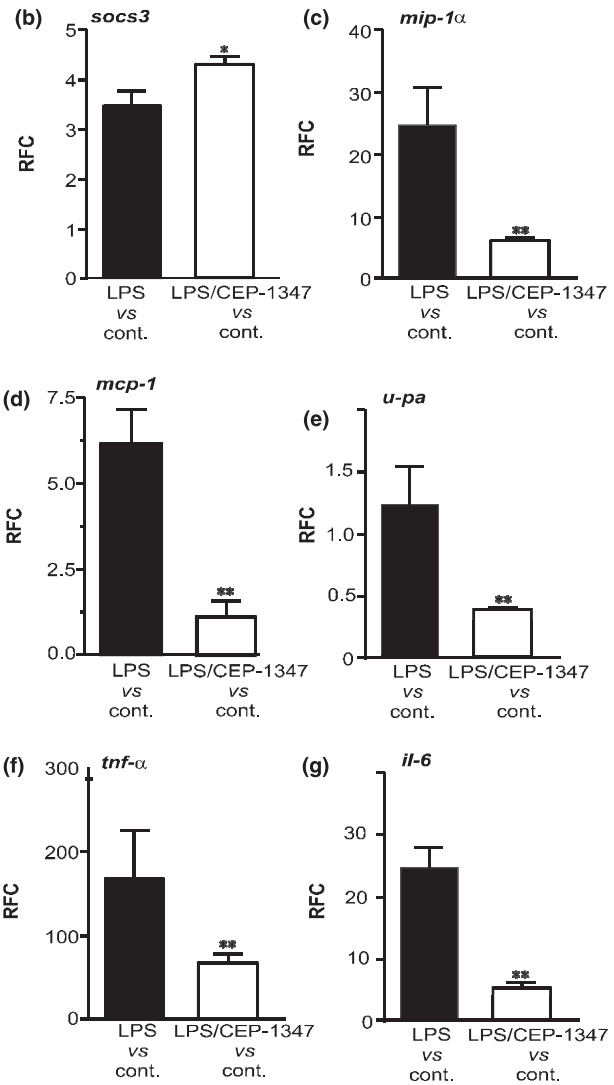

Fig. 6 The anti-inflammatory profile of CEP-1347 at the transcriptional level in LPS-stimulated microglia. BV-2 cells were treated with CEP-1347 (500 nM) for 45 min followed by LPS stimulation (100 ng/mL) for 4 h. (a) Total RNA was purified and labelled cDNA was prepared. Different competitive cDNA hybridization experiments were carried out on a small custom array for LPS versus control, and LPS versus LPS + CEP-1347. Data presented are the average of six or eight hybridizations based on two to three independent cell preparations. Genes were included if regulated ≥ 1.7-fold in either all, or all but one, of the six to eight hybridizations relating to an experiment. Shadings specify regulation by CEP-1347. Dark shading indicates up-regulation, light shading down-regulation, no shading means no regulation. (b–g) Differences in mRNA expression (normalized to GAPDH) for treated BV-2 cells regarding socs3, mip-1α, mcp-1, upa, tnf-α and Il-6 were determined by real-time PCR. Data are presented as relative fold changes (RFC) for cDNA abundances. All data are presented as means of triplicates ± SD. *$p < 0.05$, **$p < 0.01$

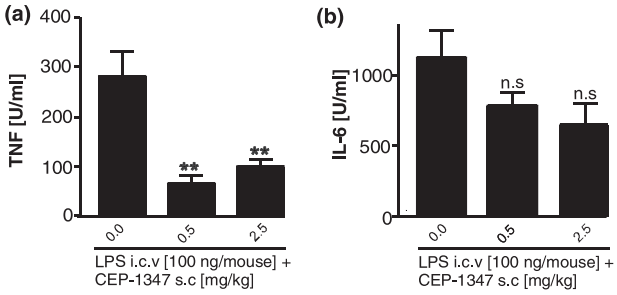

Fig. 7 Anti-inflammatory effects of CEP-1347 *in vivo*. Male CD1 mice were divided into four groups, one of which received vehicle, and two received s.c. injections of CEP-1347 (0.5 mg/kg or 2.5 mg/kg) 1 h prior to i.c.v. injection of LPS (100 ng/mouse). The fourth group was left untreated (control). Ninety minutes after i.c.v. injection, the brains were recovered, homogenized and the bioactivity of IL-6 (a) and TNF (b) was measured (see Materials and methods). Statistics were performed by comparing LPS-injected animals treated with CEP-1347 to vehicle treated. No TNF or IL-6 was detectable in the brains of mice receiving no LPS (TNF < 1 U/mL homogenate; IL-6 < 50 U/mL homogenate). Data are displayed as means ± SD ($n = 9$–10) of one experiment. $^{**}p < 0.01$.

The cause of inflammation in most neurodegenerative diseases is still poorly understood. Whereas the microglial activation in AD appears to be related to the Aβ peptide, the activation in PD continues to be elusive. However, it has been reported as coinciding temporally with the loss of dopaminergic neurons (McGeer *et al.* 1988). Even though the relevant triggers of microglial activation may not yet be identified, AD and PD treatment strategies might benefit from inclusion of an anti-inflammatory component.

In order to examine a possible effect of CEP-1347 in various settings, microglia were stimulated with a battery of inflammatory stimuli. MLK inhibitors have not previously been tested on microglia and it was therefore investigated whether the effect correlated with the known inhibitory activity of CEP-1347 on MAPK pathways. By use of phosphorylation specific antibodies, it was first established that LPS indeed activated the relevant branches of MAPK signalling (p38 and JNK/c-Jun). Consistent with the upstream position of MLKs in those pathways, it was observed that pre-incubation with CEP-1347 reduced phosphorylation of p38, JNK/c-Jun in LPS stimulated cells. By the use of an immunocytochemical approach, it was additionally verified that the decrease in c-Jun phosphorylation was reflected in diminished nuclear staining for P-c-Jun. No cytosolic staining for P-c-Jun was observed, indicating that the translocation of the phosphorylated transcription factor is very rapid, or that the majority of c-Jun resides in the nucleus in resting microglia, and then becomes phosphorylated upon stimulation.

As activated p38 and c-Jun are well-known controllers of cytokine/chemokine production in microglia, the inhibitory effect of CEP-1347 on TNF-α, IL-6 and MCP-1 production correlates well with inhibition of phosphorylation (= prevention of activation). We reasoned that the prevention of activation of inflammatory transcription factors would result in reduced mRNA levels for the targeted cytokines. Indeed, CEP-1347 treatment was found to reduce mRNA levels for tnf-α, IL-6 and chemokines 4 h after stimulation.

CEP-1347 has, up to now, been studied mostly in neuronal cells. We are not aware of studies with any cells of the macrophage lineage or other immune cells – thus, there is very little knowledge on modulation of the innate immune response. One study addressed the role of MLKs in an inflammation-like process, i.e. astrocyte activation by cytokines (Falsig *et al.* 2004b). Also in this paradigm, CEP-1347 did not affect NF-κB activation, and the microglia data shown here corroborate these findings. Dependence of NF-κB on MLK has not been indicated in a neuronal model or in any model of LPS stimulation. CEP-1347 down-regulated NO production and NOS induction in astrocytes (Falsig *et al.* 2004b), but did not show this effect in parallel experiments in microglia. Thus, regulation of iNOS induction by CEP-1347 differs between astrocytes and microglia. To our knowledge, there are no other studies addressing the modulation of NO production by CEP-1347. The iNOS promoter is extremely complex in comparison with that of other inflammatory molecules and differences between cell types and stimuli are commonly observed. With respect to JNK and p38 regulation, our data are consistent with many studies where neuronal cell types were examined.

MLKs are new players in inflammatory cell activation, but at this point it is difficult to predict whether MLK inhibitors will, in general, have a different anti-inflammatory profile than currently used compounds. We found that the effect of CEP-1347 is unrelated to direct inhibition of cyclo-oxygenase (COX) enzymes, elevation of cAMP or induction of IL-10 induction. This is in line with CEP-1347 acting differently from compounds such as NSAIDs (direct COX inhibition) (Berg *et al.* 1999), or phosphodiesterase inhibitors (increase in cAMP and IL-10 production) (Kambayashi *et al.* 1995). Additional studies regarding differences between the anti-inflammatory properties of CEP-1347 and reference compounds are under current investigation in our laboratory.

In addition to being an inhibitor in murine inflammatory models, CEP-1347 also showed effects in a human system. THP-1 cells were highly susceptible to CEP-1347 modulation of TNF-α production. Microglia are generally believed to originate from invading monocytes (mesodermal origin) (Priller *et al.* 2001). Because THP-1 cells are monocyte derived, they are likely to deviate from human microglia to some extent as the CNS environment has never primed them. We therefore tested whether CEP-1347 would also be a potent anti-inflammatory agent in a human model based on microglia isolated from post-mortem tissue. Our results

suggest that the MLKs in human monocytes, murine microglia and human microglia are important for endotoxin signalling, and that the inflammatory response is modulated by CEP-1347.

The inhibitory data on TNF-α production were confirmed *in vivo* in a murine model, demonstrating that the MLKs are also important for the transduction of inflammatory signals when microglia are activated in their natural surroundings. Controversy exists as to whether rodent astrocytes also respond to LPS and therefore also might contribute to TNF-α production. *In vitro* results from our own laboratory indicate that murine astrocytes are poor producers of TNF-α when stimulated with either LPS or a cytokine mix, but do respond to a cytokine mixture by up-regulating the astrocyte activation marker GFAP (Falsig *et al*. 2004a). Some have reported that astrocyte cultures do respond to LPS by producing NO, but this has been suggested as being due to the existence of microglia within the cultures (Vincent *et al*. 1996; Possel *et al*. 2000; Sola *et al*. 2002; rat). However, LPS-induced iNOS induction within astrocytes has also been observed (Kong *et al*. 1996; mouse). In our laboratory, we observed iNOS induction and GFAP in astrocytes under inflammatory conditions, while TNF production was not increased. In our *in vivo* model of cerebral inflammation, GFAP was not up-regulated as assessed by real-time PCR. We interpret this as sign of minimal activation of astrocytes under these conditions. The most likely source for the cytokines measured in brain homogenates appears to be microglia themselves, but at the present stage we cannot entirely exclude some contribution from astrocytes.

The contribution of inflammatory cytokines to the pathology in neurodegenerative diseases is under active investigation. A recent report suggests that patients with AD may be more susceptible to the neurotoxic properties of TNF-α as they have reduced level of the MADD protein known to inhibit induction of apoptosis induced by TNF-α binding (Del Villar and Miller 2004). Furthermore, other evidence points to IL-6 as promoting phosphorylation of the neuronal intracellular filament tau (Quintanilla *et al*. 2004). Hyperphosphorylated tau is a hallmark of AD and our finding that CEP-1347 can reduce induction of IL-6 and TNF-α is intriguing. Altogether, there is considerable evidence in favour of anti-inflammatory compounds for the treatment of AD, but it is not clear whether a monotherapy would be adequate to obtain treatment success. In addition, the manner in which inflammation is addressed is worth some consideration. Classical COX inhibitors block only a minor aspect of microglial inflammation (eicosanoid production) and hardly affect cytokine production (Berg *et al*. 1999). New anti-inflammatory/antioxidant strategies are frequently focused on inhibition of the inflammatory master regulator NF-κB (Karin *et al*. 2004), which also has anti-apoptotic functions whose inhibition may not be desirable in neurodegenerative conditions (Bhakar *et al*. 2002). In the above context, CEP-1347 seems particularly interesting because of its dual mechanism of action involving both direct neuroprotection and inhibition of inflammation.

From our initial cytokine measurements, it might be speculated that MLK inhibition by CEP-1347 would block all inflammatory genes non-specifically. However, this was not the case. CEP-1347 was found to mainly reduce the expression of secreted factors up-regulated by LPS, while it enhanced the expression of genes such as ccaat/enhancer binding protein, serum amyloid a2, serum amyloid a3, and lipocalin 2. The selective repression of a subset of genes was in line with CEP-1347 only having a minor effect on iNOS induction and nitric oxide production. This distinguishes CEP-1347 from previously mentioned anti-inflammatory drugs such as direct NF-κB inhibitors, or phophodiesterase IV inhibitors, which are reported to exert more general repression of inflammatory mediators (Beshay *et al*. 2001).

One of the essential roles of microglia in the CNS is the removal of debris/dead cells by phagocytosis. In AD, it is also likely that microglia contribute to the removal of neurotoxic Aβ plaques. Therefore, it was examined as to whether CEP-1347 would interfere with crucial microglial 'house-keeping tasks' such as phagocytosis. CEP-1347 did not affect the engulfment of bacteria by microglia. This separates the anti-inflammatory function of CEP-1347 from inhibition of basic maintenance tasks in the CNS environment, and also excludes the MLKs from having a significant role in the regulation of bacterial phagocytosis. In contrast, direct inhibition of p38 or MAPKAP kinase 2 would result in reduced phagocytosis (Lehner *et al*. 2002).

An interesting feature of the anti-inflammatory action of CEP-1347 is its site of action within the signal cascade. MLK kinases are located upstream in the p38 cascade, and constitute only some of several potential activators. Thus, by only inhibiting the MLK family, the capability of other MAPKKK to activate p38 is preserved. This may be important as p38 has been assigned important house-keeping functions in the CNS, such as contribution to synaptic plasticity shown to be blocked by direct p38 inhibition (Bolshakov *et al*. 2000; Guan *et al*. 2003). The signalling cascade upstream of p38 activation in synaptic plasticity still has to be fully clarified, but if it circumvents MLK activation, p38 activation may be spared in the presence of CEP-1347. Similar considerations apply to the JNK pathway, playing important roles in regeneration/axon growth which is not blocked by CEP-1347 (Harris *et al*. 2002)

In conclusion, we report that CEP-1347 is capable of modulating microglial inflammation by inhibiting the MLKs. The effect involves dampening of two inflammation-associated MAPK pathways (p38 and JNK), but largely spares the NF-κB system. This results in an anti-inflammatory profile that targets certain cytokines without affecting iNOS induction or phagocytic capability. This anti-inflammatory effect

of CEP-1347, or other MLK inhibitors, coupled with its neuroprotective properties, may act synergistically to affect the pathogenesis of neurodegenerative diseases.

Acknowledgements

We are indebted to A. Rassov, J. Falsig, S. Rasmussen, and Drs K. Thirstrup, J. Gerwien, J. Lotharius, J. Pedersen and J. Egebjerg for valuable contributions and insightful discussions during the course of this work. We also gratefully acknowledge the contribution by the Netherlands Brain Bank (co-ordinator Dr R. Ravid) to these studies in making available human post-mortem brain tissue. SL is the recipient of a grant by the Danish Ministry of Science, Technology and Innovation. SL, AM, DB-C, PP and ML are, or were, employees of H. Lundbeck A/S and Cephalon Inc., companies currently evaluating the clinical use of CEP1347 in the PRECEPT trial on Parkinson's disease patients.

References

Aggarwal B. B., Kohr W. J., Hass P. E., Moffat B., Spencer S. A., Henzel W. J., Bringman T. S., Nedwin G. E., Goeddel D. V. and Harkins R. N. (1985) Human tumor necrosis factor: production, purification, and characterization. *J. Biol. Chem.* **260**, 2345–2354.

Berg J., Fellier H., Christoph T., Grarup J. and Stimmeder D. (1999) The analgesic NSAID lornoxicam inhibits cyclooxygenase (COX)-1/-2, inducible nitric oxide synthase (iNOS), and the formation of interleukin (IL)-6 *in vitro*. *Inflamm. Res.* **48**, 369–379.

Beshay E., Croze F. and Prud'homme G. J. (2001) The phosphodiesterase inhibitors pentoxifylline and rolipram suppress macrophage activation and nitric oxide production *in vitro* and *in vivo*. *Clin. Immunol.* **98**, 272–279.

Bhakar A. L., Tannis L. L., Zeindler C., Russo M. P., Jobin C., Park D. S., MacPherson S. and Barker P. A. (2002) Constitutive nuclear factor-κB activity is required for central neuron survival. *J. Neurosci.* **22**, 8466–8475.

Blasi E., Barluzzi R., Bocchini V., Mazzolla R. and Bistoni F. (1990) Immortalization of murine microglial cells by a v-raf/v-myc carrying retrovirus. *J. Neuroimmunol.* **27**, 229–237.

Boll J. B., Geist M. A., Kaminski S. G., Petersen K., Leist M. and Vaudano E. (2004) Improvement of embryonic dopaminergic neurone survival in culture and after grafting into the striatum of hemiparkinsonian rats by CEP-1347. *J. Neurochem.* **88**, 698–707.

Bolshakov V. Y., Carboni L., Cobb M. H., Siegelbaum S. A. and Belardetti F. (2000) Dual MAP kinase pathways mediate opposing forms of long-term plasticity at CA3-CA1 synapses. *Nat. Neurosci.* **3**, 1107–1112.

Chen H., Zhang S. M., Hernan M. A., Schwarzschild M. A., Willett W. C., Colditz G. A., Speizer F. E. and Ascherio A. (2003) Nonsteroidal anti-inflammatory drugs and the risk of Parkinson disease. *Arch. Neurol.* **60**, 1059–1064.

Combs C. K., Karlo J. C., Kao S. C. and Landreth G. E. (2001) β-Amyloid stimulation of microglia and monocytes results in TNFα-dependent expression of inducible nitric oxide synthase and neuronal apoptosis. *J. Neurosci.* **21**, 1179–1188.

De Groot C. J., Montagne L., Janssen I., Van Ravid R. D., V. and Veerhuis R. (2000) Isolation and characterization of adult microglial cells and oligodendrocytes derived from postmortem human brain tissue. *Brain Res. Brain Res. Protoc.* **5**, 85–94.

Del Villar K. and Miller C. A. (2004) Down-regulation of DENN/MADD, a TNF receptor binding protein, correlates with neuronal cell death in Alzheimer's disease brain and hippocampal neurons. *Proc. Natl Acad. Sci. USA* **101**, 4210–4215.

Delgado M. and Ganea D. (2003) Neuroprotective effect of vasoactive intestinal peptide (VIP) in a mouse model of Parkinson's disease by blocking microglial activation. *FASEB* **17**, 944–946.

Dukic-Stefanovic S., Gasic-Milenkovic J., Deuther-Conrad W. and Munch G. (2003) Signal transduction pathways in mouse microglia N-11 cells activated by advanced glycation endproducts (AGEs). *J. Neurochem.* **87**, 44–55.

Eikelenboom P., Bate C., Van Gool W. A., Hoozemans J. J., Rozemuller J. M., Veerhuis R. and Williams A. (2002) Neuroinflammation in Alzheimer's disease and prion disease. *Glia* **40**, 232–239.

Falsig J., Latta M. and Leist M. (2004a) Defined inflammatory states in astrocyte cultures: correlation with susceptibility towards CD95-driven apoptosis. *J. Neurochem.* **88**, 181–193.

Falsig J., Porzgen P., Lotharius J. and Leist M. (2004b) Specific modulation of astrocyte inflammation by inhibition of mixed lineage kinases with CEP-1347. *J. Immunol.* **173**, 2762–2770.

Gallo K. A. and Johnson G. L. (2002) Mixed-lineage kinase control of JNK and p38 MAPK pathways. *Nat. Rev. Mol Cell. Biol.* **3**, 663–672.

Gao H. M., Hong J. S., Zhang W. and Liu B. (2002a) Distinct role for microglia in rotenone-induced degeneration of dopaminergic neurons. *J. Neurosci.* **22**, 782–790.

Gao H. M., Jiang J., Wilson B., Zhang W., Hong J. S. and Liu B. (2002b) Microglial activation-mediated delayed and progressive degeneration of rat nigral dopaminergic neurons: relevance to Parkinson's disease. *J. Neurochem.* **81**, 1285–1297.

Gao H. M., Liu B., Zhang W. and Hong J. S. (2003) Novel anti-inflammatory therapy for Parkinson's disease. *Trends Pharmacol. Sci.* **24**, 395–401.

Giovannini M. G., Scali C., Prosperi C., Bellucci A., Vannucchi M. G., Rosi S., Pepeu G. and Casamenti F. (2002) β-amyloid-induced inflammation and cholinergic hypofunction in the rat brain *in vivo*: involvement of the p38MAPK pathway. *Neurobiol. Dis.* **11**, 257–274.

Giulian D. and Baker T. J. (1986) Characterization of ameboid microglia isolated from developing mammalian brain. *J. Neurosci.* **6**, 2163–2178.

Guan Z., Kim J. H., Lomvardas S., Holick K., Xu S., Kandel E. R. and Schwartz J. H. (2003) p38 MAP kinase mediates both short-term and long-term synaptic depression in aplysia. *J. Neurosci.* **23**, 7317–7325.

Harris C. A., Deshmukh M., Tsui-Pierchala B., Maroney A. C. and Johnson E. M. J. (2002) Inhibition of the c-Jun N-terminal kinase signaling pathway by the mixed lineage kinase inhibitor CEP-1347 (KT7515) preserves metabolism and growth of trophic factor-deprived neurons. *J. Neurosci.* **22**, 103–113.

Hughes T. R., Mao M., Jones A. R. *et al.* (2001) Expression profiling using microarrays fabricated by an ink-jet oligonucleotide synthesizer. *Nat. Biotechnol.* **19**, 342–347.

Hunter C. L., Quintero E. M., Gilstrap L., Bhat N. R. and Granholm A. C. (2004) Minocycline protects basal forebrain cholinergic neurons from mu p75-saporin immunotoxic lesioning. *Eur. J. Neurosc.* **19**, 3305–3316.

Kambayashi T., Jacob C. O., Zhou D., Mazurek N., Fong M. and Strassmann G. (1995) Cyclic nucleotide phosphodiesterase type IV participates in the regulation of IL-10 and in the subsequent inhibition of TNF-α and IL-6 release by endotoxin-stimulated macrophages. *J. Immunol.* **155**, 4909–4916.

Kaneko M., Saito Y., Saito H. *et al.* (1997) Neurotrophic 3,9-bis[(alkylthio) methyl]-and-bis (alkoxymethyl)-K-252a derivatives. *J. Med. Chem.* **40**, 1863–1869.

Karin M., Yamamoto Y. and Wang Q. M. (2004) The IKK NF-κB system: a treasure trove for drug development. *Nat. Rev. Drug Discov.* **3**, 17–26.

Kim S. H., Smith C. J. and Van Eldik L. J. (2004) Importance of MAPK pathways for microglial pro-inflammatory cytokine IL-1β production. *Neurobiol. Aging* **25**, 431–439.

Kingham P. J. and Pocock J. M. (2000) Microglial apoptosis induced by chromogranin A is mediated by mitochondrial depolarisation and the permeability transition, but not by cytochrome c release. *J. Neurochem.* **74**, 1452–1462.

Kingham P. J. and Pocock J. M. (2001) Microglial secreted cathepsin B induces neuronal apoptosis. *J. Neurochem.* **76**, 1475–1484.

Knudsen S. (2002) *A Biologist's Guide to Analysis of CDNA Microarray Data*, Wiley Interscience, New York.

Kong L. Y., McMillian M. K., Maronpot R. and Hong J. S. (1996) Protein tyrosine kinase inhibitors suppress the production of nitric oxide in mixed glia, microglia-enriched or astrocyte-enriched cultures. *Brain Res.* **729**, 102–109.

Kurkowska-Jastrzebska I., Wronska A., Kohutnicka M., Czlonkowski A. and Czlonkowska A. (1999) The inflammatory reaction following 1-methyl-4-phenyl-1,2,3, 6-tetrahydropyridine intoxication in mouse. *Exp. Neurol.* **156**, 50–61.

Lehner M. D., Schwoebel F., Kotlyarov A., Leist M., Gaestel M. and Hartung T. (2002) Mitogen-activated protein kinase-activated protein kinase 2-deficient mice show increased susceptibility to *Listeria* monocytogenes infection. *J. Immunol.* **168**, 4667–4673.

Lipton J. M., Macaluso A., Hiltz M. E. and Catania A. (1991) Central administration of the peptide α-MSH inhibits inflammation in the skin. *Peptides* **12**, 795–798.

Maroney A. C., Finn J. P., Bozyczko-Coyne D., O'Kane T. M., Neff N. T., Tolkovsky A. M., Park D. S., Yan C. Y., Troy C. M. and Greene L. A. (1999) CEP-1347 (KT7515), an inhibitor of JNK activation, rescues sympathetic neurons and neuronally differentiated PC12 cells from death evoked by three distinct insults. *J. Neurochem.* **73**, 1901–1912.

Maroney A. C., Glicksman M. A., Basma A. N. *et al.* (1998) Motoneuron apoptosis is blocked by CEP-1347 (KT 7515), a novel inhibitor of the JNK signaling pathway. *J. Neurosci.* **18**, 104–111.

Maroney A. C., Finn J. P., Connors T. J. *et al.* (2001) Cep-1347 (KT7515), a semisynthetic inhibitor of the mixed lineage kinase family. *J. Biol. Chem.* **276**, 25 302–25 308.

McGeer E. G. and McGeer P. L. (2003) Inflammatory processes in Alzheimer's disease. *Prog. Neuropsychopharmacol. Biol. Psychiatry* **27**, 741–749.

McGeer P. L., Itagaki S., Boyes B. E. and McGeer E. G. (1988) Reactive microglia are positive for HLA-DR in the substantia nigra of Parkinson's and Alzheimer's disease brains. *Neurology* **38**, 1285–1291.

McGeer P. L., McGeer E., Rogers J. and Sibley J. (1990) Anti-inflammatory drugs and Alzheimer disease. *Lancet* **335**, 1037.

Morath S., Geyer A. and Hartung T. (2001) Structure–function relationship of cytokine induction by lipoteichoic acid from *Staphylococcus aureus*. *J. Exp. Med.* **193**, 393–397.

Munch G., Gasic-Milenkovic J., Dukic-Stefanovic S., Kuhla B., Heinrich K., Riederer P., Huttunen H. J., Founds H. and Sajithlal G. (2003) Microglial activation induces cell death, inhibits neurite outgrowth and causes neurite retraction of differentiated neuroblastoma cells. *Exp. Brain Res.* **150**, 1–8.

Nakajima K., Tohyama Y., Kohsaka S. and Kurihara T. (2004) Protein kinase Cα requirement in the activation of p38 mitogen-activated protein kinase, which is linked to the induction of tumor necrosis factor α in lipopolysaccharide-stimulated microglia. *Neurochem. Int.* **44**, 205–214.

Possel H., Noack H., Putzke J., Wolf G. and Sies H. (2000) Selective upregulation of inducible nitric oxide synthase (iNOS) by lipopolysaccharide (LPS) and cytokines in microglia: *in vitro* and *in vivo* studies. *Glia* **32**, 51–59.

Priller J., Flugel A., Wehner T. *et al.* (2001) Targeting gene-modified hematopoietic cells to the central nervous system: use of green fluorescent protein uncovers microglial engraftment. *Nat. Med.* **7**, 1356–1361.

Quintanilla R. A., Orellana D. I., Gonzalez-Billault C. and Maccioni R. B. (2004) Interleukin-6 induces Alzheimer-type phosphorylation of tau protein by deregulating the cdk5/p35 pathway. *Exp. Cell Res.* **295**, 245–257.

Saporito M. S., Brown E. M., Miller M. S. and Carswell S. (1999) CEP-1347/KT-7515, an inhibitor of c-jun N-terminal kinase activation, attenuates the 1-methyl-4-phenyl tetrahydropyridine-mediated loss of nigrostriatal dopaminergic neurons *in vivo*. *J. Pharmacol. Exp. Ther.* **288**, 421–427.

Sironi M., Breviario F., Proserpio P., Biondi A., Vecchi A., Van Damme J., Dejana E. and Mantovani A. (1989) IL-1 stimulates IL-6 production in endothelial cells. *J. Immunol.* **142**, 549–553.

Sola C., Casal C., Tusell J. M. and Serratosa J. (2002) Astrocytes enhance lipopolysaccharide-induced nitric oxide production by microglial cells. *Eur. J. Neurosci.* **16**, 1275–1283.

Suzuki T., Hide I., Ido K., Kohsaka S., Inoue K. and Nakata Y. (2004) Production and release of neuroprotective tumor necrosis factor by P2X7 receptor-activated microglia. *J. Neurosci.* **24**, 1–7.

Vincent V. A., Van Dam A. M., Persoons J. H., Schotanus K., Steinbusch H. W., Schoffelmeer A. N. and Berkenbosch F. (1996) Gradual inhibition of inducible nitric oxide synthase but not of interleukin-1β production in rat microglial cells of endotoxin-treated mixed glial cell cultures. *Glia* **17**, 94–102.

Xu Z., Maroney A. C., Dobrzanski P., Kukekov N. V. and Greene L. A. (2001) The MLK family mediates c-Jun N-terminal kinase activation in neuronal apoptosis. *Mol. Cell Biol.* **21**, 4713–4724.

Yan Q., Zhang J., Liu H., Babu-Khan S., Vassar R., Biere A. L., Citron M. and Landreth G. (2003) Anti-inflammatory drug therapy alters β-amyloid processing and deposition in an animal model of Alzheimer's disease. *J. Neurosci.* **23**, 7504–7509.